Published in final edited form as:
Hepatology. 2015 February ; 61(2): 648–659. doi:10.1002/hep.27387.

Chronic Passive Venous Congestion drives Hepatic Fibrogenesis via Sinusoidal Thrombosis and Mechanical Forces

Douglas A Simonetto[1], **Hui-yin Yang**[1,2], **Meng Yin**[3], **Thiago M de Assuncao**[1], **Jung Hee Kwon**[1], **Moira Hilsher**[4], **Shuchong Pan**[5], **Liu Yang**[1], **Yan Bi**[1], **Arthur Beyder**[1], **Sheng Cao**[1], **Robert D Simari**[5], **Richard Ehman**[3], **Patrick S Kamath**[1], and **Vijay H Shah**[1]

[1]Gastroenterology Research Unit, Mayo Clinic, Rochester, MN

[2]Chinese PLA General Hospital & Chinese PLA Medical School; Integrative Medical Center of the 302 Military Hospital, Beijing, People's Republic of China

[3]Department of Radiology, Mayo Clinic, Rochester, MN

[4]Department of Medicine, Mayo Clinic, Rochester, MN, United States

[5]Cardiovascular Diseases, Mayo Clinic, Rochester, MN, United States.

Abstract

Chronic passive hepatic congestion (congestive hepatopathy) leads to hepatic fibrosis; however the mechanisms involved in this process are not well understood. We developed a murine experimental model of congestive hepatopathy through partial ligation of the inferior vena cava (pIVCL). C57BL/6 and transgenic mice overexpressing tissue factor pathway inhibitor (SM22α - TFPI) were subjected to pIVCL or SHAM. Liver and blood samples were collected and analyzed in immunohistochemical, morphometric, real-time polymerase chain reaction and western blot assays. Hepatic fibrosis and portal pressure were significantly increased after pIVCL concurrent with hepatic stellate cell (HSC) activation. Liver stiffness, as assessed by magnetic resonance elastography, correlated with portal pressure and preceded fibrosis in our model. Hepatic sinusoidal thrombosis as evidenced by fibrin deposition was demonstrated both in mice after pIVCL as well as in humans with congestive hepatopathy. Warfarin treatment and TFPI overexpression both had a protective effect on fibrosis development and HSC activation after pIVCL. *In vitro* studies show that congestion stimulates HSC fibronectin (FN) fibril assembly through direct effects of thrombi as well as by virtue of mechanical strain. Pretreatment with either Mab13 or Cytochalasin-D, to inhibit β-integrin or actin polymerization, respectively, significantly reduced fibrin and stretch induced FN fibril assembly.

Conclusion—Chronic hepatic congestion leads to sinusoidal thrombosis and strain, which in turn promote hepatic fibrosis. These studies mechanistically link congestive hepatopathy to hepatic fibrosis.

Address for correspondence: Vijay H Shah, MD Mayo Clinic 200 First ST SW Rochester, MN 55905 Ph: (507) 255-6028/Fax: (507) 255-6318 shah.vijay@mayo.edu.

Keywords

Congestive hepatopathy; Extracellular Matrix; mechanical stretch; hepatic stellate cell; fibronectin fibril assembly

INTRODUCTION

Congestive heart failure and Budd-Chiari syndrome encompass a group of disorders that impair hepatic venous outflow and lead to hepatic congestion. Chronic hepatic congestion, also termed congestive hepatopathy, subsequently leads to hepatic fibrosis. This phenomenon is nowadays more frequently observed owing to increasing prevalence of chronic heart failure in an aging population(1). Additionally, surgical procedures, developed for correction of complex congenital heart defects, has markedly increased the life expectancy of patients with severe congenital heart disease(2) but now predisposes this population to congestive hepatopathy and its sequelae(3). In contrast to canonical inflammatory pathways that drive hepatic fibrogenesis in conditions such as viral hepatitis, little is known about how chronic hepatic congestion leads to fibrosis.

Retrospective observations of *ex vivo* human liver specimens of patients with hepatic congestion has led to the hypothesis of parenchymal extinction(4, 5). In this model, congestion and reduced cardiac output lead to hepatocyte ischemia, which triggers the fibrotic response. This and other models by which hepatic congestion leads to fibrosis have not been tested experimentally. Further advances in our understanding of the pathogenesis of this condition have been hampered in part by lack of appropriate experimental models in which hepatic congestion can be studied in context of easily implemented molecular perturbations and genetic modifications.

In this study, we developed as well as characterized a model of congestive hepatopathy in mice. We describe distinctive fibrogenic mechanisms secondary to chronic congestion as opposed to those conferred by traditional biliary or hepatocellular insults. We demonstrate marked fibrin deposits and alpha-smooth muscle actin (α-SMA) expression in areas of hepatic fibrosis in this murine model as well in liver specimens of patients with congestive liver diseases. Furthermore, our results show that disruption of the coagulation cascade, through pharmacologic and molecular approaches reduces congestion related fibrosis. These observations led us to investigate the direct and indirect effects of thrombi on FN fibril assembly by hepatic stellate cells (HSC), an early step in extracellular matrix maturation and fibrosis development. These studies show that both fibrin as well as mechanical vascular strain conferred by congestion, stimulate FN fibril assembly. In total, these studies elucidate mechanisms linking congestive hepatopathy to fibrosis, highlight a potential beneficial role for anticoagulation in this condition, and uncover findings that may have broader applicability to other causes of liver fibrosis.

METHODS

See Supplementary Methods for more details.

Partial inferior vena cava ligation

A 2 cm incision was made just below the xiphoid process and along the lower costal margin of the mice. Under sterile techniques, the falciform ligament was divided and the suprahepatic IVC was exposed using sterile cotton tipped applicator. The IVC was circumferentially isolated and a sterile steel wire of 0.6 mm in diameter was placed on the anterior surface of the IVC. A 6.0 silk thread was then tightly tied around both the IVC and the wire, which was subsequently gently removed. The diameter of 0.6 mm was chosen to reduce the IVC diameter by approximately 70% based on a series of pilot studies performed with varying alternative diameters. Sham operation included all the steps above except for the ligation. Mice were sacrificed 2, 4 or 6 weeks postoperatively.

SM22α -TFPI mice

Transgenic mice overexpressing tissue factor pathway inhibitor (TFPI) via the smooth muscle–specific promoter SM22 (SM22α-TFPI) have been described previously (6). The mice were maintained on C57/Bl6 background. Age-matched (10-12 weeks) C57/Bl6 mice (wild-type [WT]) were used as controls in all experiments.

Deoxycholic Acid (DOC) Solubility Assays

Biotinylated fibronectin (b-FN) was generated as directed by the manufacturer (EZ-link Sulfo-NHS-Biotin; Thermo Scientific) and previously described (7). For fibrin experiments, serum-starved HSC were plated on fibrinogen-, fibrin- or collagen- coated or uncoated dishes for 4 hours. Thrombin (0.2 U) was added to serum-free media of cells plated on the uncoated dishes. After attachment, cells were washed and serum-free DMEM containing b-FN (10 or 50 μg) was added for 6 hours. For stretch experiments, serum-starved HSC were stretched for 6 hours after b-FN was added. In some experiments cells were pre-treated with rat anti-human CD29 (Mab13; 1:200) or cytochalasin D (1:1000) for 30 minutes. The cells were then lysed in 2% DOC lysis buffer (2% DOC, 20mM tris-CL pH 8.8, 2mM PMSF, 2mM EDTA, 2mM iodoacetic acid, and 2 mM N-ethylmaleimide) and lysates were passed through a 25 gauge needle and centrifuged (16,000 × g, 20 min) at 4°C. The supernatant was removed and saved as the DOC soluble fraction, while the pellet was re-suspended in 2X SDS reducing sample buffer (Invitrogen). Protein levels were determined for DOC soluble fractions by BCA assay (Pierce). Equal amounts of DOC-soluble and -insoluble protein were resolved on a 4–12% SDS-PAGE gel.

Magnetic Resonance Elastography (MRE)

All *in vivo* animal experiments and fibrin gel studies were implemented on a 3.0-T whole-body GE imager (HDx, GE Healthcare, Milwaukee, WI), using a custom birdcage coil. A silver needle is used to generate shear waves throughout the liver in mice. The mice were anesthetized with 1.0-1.5% isoflurane. MRE wave images were acquired with a multifrequency 3-D/3-axis EPI MRE sequence (120, 200Hz) with a resolution of 0.3×0.3×2 mm^3. For fibrin gel studies, a torsional vibration of 200Hz was used to vibrate two vials (with and without cells embedded) simultaneously to generate cylindrical shear wave field in the fibrin gels. MRE images were inverted with a 3D direct inversion of the Helmholtz equation to calculate the complex shear modulus. All quantities were reported as means and

standard deviations of ROIs drawn to encompass as much of the liver as possible that had significant wave propagation.

Human subjects

Liver samples from healthy individuals and from patients with congestive heart failure or with previous surgical procedures for congenital heart disease were obtained from clinically indicated biopsy and/or surgical waste under institutional review board– approved protocols were used for histochemical studies. Patient demographics are detailed on Supplementary Tables 1 and 2.

RESULTS

Characterization of a Murine Model of Congestive Fibrosis by Partial Ligation of the Inferior Vena Cava

To simulate human congestive hepatopathy, we developed a surgical model of hepatic venous outflow obstruction in mice through partial ligation of the suprahepatic abdominal inferior vena cava (pIVCL) (Fig. 1A and Supp Fig. 1). Gross examination of the liver after pIVCL showed alternate dark red and pale areas, resembling a “nutmeg” appearance. H&E staining of liver sections revealed areas of centrilobular necrosis, vascular extravasation and sinusoidal dilatation, consistent with hepatic histologic characteristics in humans with congestive hepatopathy (8) (Fig. 1B). Next, we investigated whether chronic congestion would induce portal hypertension and liver fibrosis. At 6 weeks postoperatively the animals in the pIVCL group showed a significant increase in portal pressure (PP) and spleen-body weight ratio compared to SHAM operation (Fig. 1C). As reduced cardiac output has been suggested to contribute to ischemic hepatic injury in congestive hepatopathy we performed a 2D-echocardiogram for noninvasive assessment of cardiac hemodynamics after pIVCL. There was significant increase in heart rate, but no difference was found on left ventricular ejection fraction or cardiac output after partial IVC ligation compared to controls (Supp Fig. 2). These findings exclude the effects of reduced cardiac output in the pIVCL model. HSC activation after pIVCL was also observed based on a significant increase in the mRNA levels of hepatic α-SMA, pro-collagen 1α1, FN and TIMP-1, and immunostaining and western blot for α-SMA, compared to SHAM (Fig. 1D, E). Picro-Sirius red staining and hydroxyproline assays indicated a marked increase in collagen deposition in the liver after pIVCL compared to control (Fig. 1F), demonstrating the development of fibrosis in this experimental model of congestive hepatopathy. Immunostaining for α-SMA and collagen exhibited a centrilobular and perisinusoidal distribution, consistent with histological findings in human hepatic congestion (8, 9).

While chronic inflammation is a canonical driver of tissue fibrosis in many forms of liver injury and ensuing fibrosis (10), its role in congestive hepatopathy is not well defined. Therefore, we determined whether inflammation as measured by histologic and serologic criteria was present after pIVCL. Hepatic expression of proinflammatory cytokines did not change or only modestly increased after pIVCL, in contrast with a robust increase of these inflammatory markers after bile duct ligation, a traditional experimental model of biliary fibrosis (Supp Fig. 3). Serum alanine aminotransferase (ALT) and aspartate

aminotransferase (AST), total and indirect bilirubin as well as lipopolysaccharide-binding protein (LPS-BP), a surrogate for innate immunity, also did not significantly change after pIVCL compared to controls (Supp Fig. 4). Histologically, minimal inflammatory infiltrates were detected in liver after pIVCL, in contrast with marked hepatic inflammatory cell infiltration seen after BDL (Supp Fig. 5). Thus, there is minimal necroinflammatory activity after pIVCL, consistent with histologic and serologic findings in humans with congestive liver disease that describe bland hepatic inflammation in this condition (9, 11).

Anticoagulation Disrupts Congestive Fibrosis

Given the lack of meaningful hepatic inflammation in our model, we pursued alternative mechanisms which could be important for fibrosis development during liver congestion. Hepatic sinusoidal thrombosis has been reported in autopsies of patients with congestive heart failure and associated with areas of parenchymal extinction and fibrosis (4). To explore this concept further, we evaluated fibrin, which is present in both provisional and fully constituted clots. Fibrin was significantly increased in the liver after pIVCL compared to controls, and sinusoidal fibrin deposits were spatially associated with α-SMA expression (Fig. 2A), suggesting a potential role of thrombosis in HSC activation. Therefore, we sought to determine the importance of intrahepatic microvascular thrombosis in the development of congestion-related fibrosis by disrupting the coagulation cascade. First, we administered warfarin to mice via drinking water for 6 weeks after pIVCL. The dose of warfarin was based on a previous study (12) and then titrated in pilot experiments to achieve an International normalized ratio (INR) of approximately 2 times the baseline level of controls (Fig. 2B). Portal pressure did not change in the warfarin treated group; however spleen/body and liver/body ratios were significantly reduced in comparison with the untreated pIVCL group (Fig. 2B). There was also a significant reduction of intrahepatic fibrin levels after warfarin treatment based on immunostaining, confirming the anticipated anticoagulant effect of warfarin (Fig. 2C, top). Warfarin-treated mice also had a significant reduction in the activation of HSC, as demonstrated by α-SMA immunostaining (Fig. 2C, bottom). Finally, warfarin was protective against development of congestive fibrosis as shown by significant reduction in collagen content in the liver, both by Sirius red staining and hydroxyproline assay (Fig. 2D). These studies indicate that intrahepatic thrombosis may promote fibrosis during congestive hepatopathy.

To corroborate these pharmacological results using molecular approaches, we next evaluated whether genetic disruption of the tissue-factor dependent coagulation cascade would protect against congestive fibrosis. Tissue factor pathway inhibitor is a plasma Kunitz-type serine protease inhibitor of the TF–FVII/FVIIa complex, and therefore an endogenous inhibitor of the extrinsic coagulation pathway(13). pIVCL was performed in a transgenic mouse in which tissue factor pathway inhibitor (TFPI) is overexpressed via the smooth muscle-specific promoter SM22α (SM22α-TFPI) so as to achieve elevated systemic levels of TFPI (14). SM22α-TFPI mice showed a significant reduction of intrahepatic microvascular thrombosis (fibrin immunostaining and protein level, Fig. 3A, B). This was associated with a reduction in HSC activation (α-SMA immunostaining and protein level Fig. 3A, B) and hepatic fibrosis (Sirius red staining and hydroxyproline assay; Fig. 3C). Portal pressure and

spleen/body ratio were not significantly reduced (Fig. 3D). These findings further support the causative role of thrombosis in congestion-related hepatic fibrogenesis.

Fibrin Stimulates FN Fibril Assembly by HSC

In the final step of the coagulation cascade, circulating fibrinogen is cleaved by thrombin, a potent plasma protease, to form mature fibrin clots (15). Formation of a fibrin is the first step in the assembly of a provisional extracellular matrix, which is followed by deposition and fibrillogenesis of plasma or cellular FN (16, 17). To further elucidate the potential mechanisms by which intrahepatic thrombi could lead to liver fibrosis we next investigated the effects of fibrin on HSC. The role of thrombin in myofibroblastic differentiation of HSCs has been previously demonstrated (18), and confirmed here by increase α-SMA, FN, pro-collagen 1α1 and TIMP1 mRNA expression *in vitro* (Supp Fig. 6). Fibrin, however, does not demonstrate the same effect (Supp Fig. 7). *In vivo*, we found that fibrin co-localizes with FN suggesting interactions of these molecules at sites of congestion-related injury (Fig. 4A). Therefore, we next evaluated the effect of fibrin on FN assembly into insoluble fibrils by HSCs. FN fibril assembly is a complex process that initiates with FN binding to integrins, mainly α5β1 integrin, followed by cytoskeletal rearrangements and Rho-dependent cellular contraction (19). Through the addition of exogenous b-FN, we found that fibrin stimulates FN assembly by HSC (Fig. 4B). As fibrin is generated *in situ* by the addition of thrombin to soluble fibrinogen, we evaluated the effect of both these components separately and found the effect on FN fibril assembly to be specific to fibrin (Fig. 4B). Inhibition of β1 integrin or actin polymerization significantly reduced fibril assembly by HSCs in response to fibrin (Fig. 4C). Thus, fibrin stimulates FN fibril assembly in an actin and integrin dependent manner. Finally, to further evaluate the importance of FN fibril assembly in ECM maturation we measured the stiffness of fibrin matrix by MR elastography. Addition of HSCs to fibrin matrices significantly increased stiffness *in vitro*, and this effect was completely blocked by inhibition of β1 integrin and actin polymerization (Fig. 4D).

Mechanical Forces Stimulate FN Fibril Assembly by HSC

Liver stiffness may be increased in chronic passive congestion in humans even in the absence of advanced fibrosis (20, 21). We evaluated this concept in our model by obtaining MR elastography in mice 2, 4 and 6 weeks after pIVCL (Fig. 5A). Liver stiffness correlated with portal pressure, a surrogate for hepatic congestion, in the absence of fibrosis at 2 and 4 weeks (Fig. 5B). Liver stiffness and portal pressure were significantly elevated as early as 2 weeks postoperatively, whereas fibrosis was only markedly present at 6 weeks post-pIVCL (Fig. 5C-E). We did not observe further increase in stiffness or portal pressure at 6 weeks, and this may be a reflection that congestion rather than fibrosis drives this phenotype in this model. Therefore, stiffness may not only be a measurement of fibrosis and ECM deposition but may also detect mechanical tension generated by vascular strain in congestion. Increased intrahepatic pressure (stress) likely results in a stretch of endothelial cells and adjacent HSC, as physically reflected by sinusoidal dilatation (strain), a hallmark feature of congestive hepatopathy. While extracellular matrix stiffness regulates HSC behavior (7, 22, 23), the effects of mechanical strain on HSC remain unclear. “Pulsatile liver” a common physical finding in congestive liver conditions, particularly tricuspid regurgitation and constrictive pericarditis, illustrates this concept in the form of cyclic strain (24). We therefore evaluated

the effect of mechanical cyclic strain on HSC. Interestingly, cyclic stretch significantly increased FN secretion from HSCs (Fig. 6A). Additionally, cyclic stretch markedly increased FN fibril assembly (Fig. 6B, C). Inhibition of β1 integrin or actin polymerization also significantly reduced fibril assembly in response to stretch (Fig. 6D and E, respectively). Thus, mechanical forces such as sinusoidal stretch conferred by congestion lead to early steps of provisional matrix development.

Intrahepatic microvascular thrombosis is increased in patients with congestive hepatopathy

Liver samples were obtained from healthy individuals (controls) and from patients with congestive hepatopathy secondary to corrective surgery (Fontan procedure) for complex congenital heart disease or acquired congestive heart failure. Patients with Fontan physiology were markedly younger than acquired congestive heart failure patients (Supp Table 1 and 2). Through fibrin immunostaining we demonstrated an increase in sinusoidal thrombosis in congestive hepatopathy compared to healthy livers (Fig. 7A, upper panel). This was associated with an increase in HSC activation, as assessed by α-SMA expression (Fig. 7A, lower panel), and in liver fibrosis (Fig. 7B).

DISCUSSION

In contrast to the canonical inflammatory pathways that drive hepatic fibrogenesis in most experimental models of fibrosis and in patients with hepatitis associated fibrosis, little is known about fibrogenic mechanisms associated with congestive liver diseases. The present study makes a number of novel observations that extend our nascent understanding of this syndrome. Using a newly characterized murine model, we identify that sinusoidal congestion leads to fibrosis not through an inflammation mediated pathway but rather through sinusoidal thrombosis and mechanical strain (Fig. 8). Evidence that anticoagulation may have beneficial effects in this model also sets the stage for further human investigation to test for potential clinical benefit of anticoagulation in various forms of congestive hepatopathy.

Much of our current understanding of the pathophysiological grounds of congestive hepatopathy is based on descriptive human pathological case series. A recent series of patients, with longstanding congestive hepatopathy following surgical correction for congenital heart disease, demonstrated minimal inflammatory changes and a lack of overt hepatocellular injury in liver biopsy specimens, despite accentuated hepatic fibrosis(11). Additionally, a previous autopsy study of livers from patients with congestive heart failure demonstrated sinusoidal thrombi in proximity with areas of fibrosis and suggested a causative role of intrahepatic thrombosis for ensuing fibrosis (4). The pathogenic relevance of these findings however was indeterminate and was a focus of our present study. Histological review of our liver specimens from patients with congestive hepatopathy revealed similarities to these prior studies as we also noted dense fibrosis with a dearth of inflammatory infiltrates. The histopathological findings in our experimental model of hepatic congestion are also reminiscent of those observed in human hepatic congestion including sinusoidal dilation, red blood cell extravasation into the parenchyma and

perisinusoidal and centrilobular fibrosis (25). These findings suggested potential links between sinusoidal congestion and hepatic fibrosis which we mechanistically pursued.

Sinusoidal stasis and congestion promote fibrin formation and deposition in the liver. In fact fibrin has been implicated in the wound healing response (26) and alcohol-induced liver injury (27) although evidence for direct biological effects of fibrin on HSC is lacking. In congestive hepatopathy, sinusoidal congestion may lead to enlarged fenestrae and increased permeability allowing extravasation of blood cells and clot proteins into the space of Disse leading to direct access of fibrin to HSC (28). Our *in vitro* studies show that fibrin stimulates HSC mediated FN fibril assembly, a process in which soluble FN is converted into an insoluble fibrillar network. Some, though not all, studies indicate that FN fibril assembly is an essential step in the generation of a provisional matrix that ultimately contributes to maturation to a collagen based matrix (29). The process of FN fibril assembly requires binding of FN with α5ß1 integrin as well as actin polymerization dependent cell contraction(19). Indeed, inhibition of both these steps attenuates thrombus associated FN fibril assembly as we show here and as we and others have shown previously in response to other stimuli (7, 19).

Hepatic sinusoidal dilatation that occurs in response to congestive hepatopathy generates mechanical forces in the sinusoids and we hypothesized that these forces may contribute to HSC activation in chronic hepatic congestion. Indeed, mechanical forces play a protean role in regulation of sinusoidal vascular cells such as endothelial cells and pericytic HSC. For example, mechanical rigidity promotes HSC activation and FN fibril assembly (7, 23, 30, 31). While liver stiffness is applied as a surrogate for rigidity of extracellular matrix, it also results from elevated intrahepatic tension secondary to vascular congestion and strain. We demonstrated this concept through MR elastography, an increasingly recognized tool for detection of stiffness (21), thereby further highlighting a potential clinical utility of MRE in this condition. Congestion can lead to a “pulsatile” liver due to the associated mechanical cyclic strain imparted upon the vessel(32). Indeed, cyclic stretch promoted FN release and fibril assembly in the present studies thereby also linking congestion to fibrosis through mechanical force.

Prior dogma that cirrhosis is solely a bleeding diathesis appears to be overly simplistic. Indeed, increasing evidence indicates that cirrhosis may actually be associated with a clotting diathesis. In fact, recent studies indicate that anticoagulation may have a beneficial effect in patients with cirrhosis and in preclinical models (12, 33, 34). The protective effects of warfarin and TFPI overexpression that we observed in the pIVCL model further support this evolving concept. The mechanistic focus on TFPI has important therapeutic implications since administration of recombinant TFPI may bind to heparinoids on the sinusoidal endothelial cell surface (35). This could theoretically provide liver- and sinusoid-selective effects of exogenous TFPI administration and minimize systemic adverse effects. Considering the increasing evidence that chronic liver disease may be associated with a clotting diathesis, it is tempting to speculate that the sinusoidal thrombosis that we observed in the present study may contribute to fibrosis progression in various liver injuries beyond that observed in congestive hepatopathy. Moreover, many other proteins in the coagulation

and fibrinolytic cascades may have a role in hepatic fibrogenesis and this is an area that needs to be further explored.

While experimental animal models that emulate hepatocellular and biliary injury have been previously characterized, pre-clinical models of congestive hepatopathy have been lacking, thus hampering progress in this increasingly prevalent condition. In this study we have developed and characterized a novel murine model of hepatic venous outflow obstruction through partial ligation of the suprahepatic inferior vena cava. The present model with its expansive characterization has a number of advantages over the few previous analyses that have been reported in this arena (36). The pIVCL model uses a defined ligation that is reproducible and upon adequate training, can be performed in mice, allowing for the mechanistic, cost, and genetic advantages that accompany murine models. Importantly, both the pathologic and hemodynamic characteristics of this murine model emulate human disease based on our comparison of histology in the murine model and in human specimens acquired from patients following corrective procedures for congenital heart disease and congestive heart failure. The development of portal hypertension preceding fibrosis in this model also allows for the study of endothelial dysfunction in this condition (37) and its role in fibrogenesis. The present studies utilize this model to identify fibrin thrombi and mechanical forces as mechanistic links between hepatic congestion and matrix maturation that leads to fibrosis. They also set the stage for future work in this area that can further explore the role of anticoagulation in congestive hepatopathy.

Supplementary Material

Refer to Web version on PubMed Central for supplementary material.

Acknowledgements

The authors thank Helen I. Hendrickson, Theresa J. Johnson, Frederico Franchi and the Clinical Core of the Mayo Clinic Center for Cell Signaling in Gastroenterology (P30DK084567) for their contributions to this work.

Grant Support: Supported by National Institutes of Health (NIH) grants DK59015 and AA021171.

REFERENCES

1. Ahmed A. American College of Cardiology/American Heart Association Chronic Heart Failure Evaluation and Management guidelines: relevance to the geriatric practice. Journal of the American Geriatrics Society. 2003; 51:123–126. [PubMed: 12534856]
2. de Leval MR, Deanfield JE. Four decades of Fontan palliation. Nature reviews. Cardiology. 2010; 7:520–527.
3. Asrani SK, Asrani NS, Freese DK, Phillips SD, Warnes CA, Heimbach J, Kamath PS. Congenital heart disease and the liver. Hepatology. 2012; 56:1160–1169. [PubMed: 22383293]
4. Wanless IR, Liu JJ, Butany J. Role of thrombosis in the pathogenesis of congestive hepatic fibrosis (cardiac cirrhosis). Hepatology. 1995; 21:1232–1237. [PubMed: 7737628]
5. Wanless IR, Wong F, Blendis LM, Greig P, Heathcote EJ, Levy G. Hepatic and portal vein thrombosis in cirrhosis: possible role in development of parenchymal extinction and portal hypertension. Hepatology. 1995; 21:1238–1247. [PubMed: 7737629]
6. Pan S, Kleppe LS, Witt TA, Mueske CS, Simari RD. The effect of vascular smooth muscle cell-targeted expression of tissue factor pathway inhibitor in a murine model of arterial thrombosis. Thrombosis and haemostasis. 2004; 92:495–502. [PubMed: 15351845]

7. Yaqoob U, Cao S, Shergill U, Jagavelu K, Geng Z, Yin M, de Assuncao TM, et al. Neuropilin-1 stimulates tumor growth by increasing fibronectin fibril assembly in the tumor microenvironment. Cancer research. 2012; 72:4047–4059. [PubMed: 22738912]
8. Moschcowitz E. The morphology and pathogenesis of cardiac fibrosis of the liver. Annals of internal medicine. 1952; 36:933–955. [PubMed: 14915373]
9. Dunn GD, Hayes P, Breen KJ, Schenker S. The liver in congestive heart failure: a review. The American journal of the medical sciences. 1973; 265:174–189. [PubMed: 4573728]
10. Bissell DM. Inflammation and hepatic fibrosis. Seminars in liver disease. 2010; 30:211–214. [PubMed: 20665373]
11. Kendall TJ, Stedman B, Hacking N, Haw M, Vettukattill JJ, Salmon AP, Cope R, et al. Hepatic fibrosis and cirrhosis in the Fontan circulation: a detailed morphological study. Journal of clinical pathology. 2008; 61:504–508. [PubMed: 17965217]
12. Anstee QM, Goldin RD, Wright M, Martinelli A, Cox R, Thursz MR. Coagulation status modulates murine hepatic fibrogenesis: implications for the development of novel therapies. Journal of thrombosis and haemostasis : JTH. 2008; 6:1336–1343. [PubMed: 18485088]
13. Lwaleed BA, Bass PS. Tissue factor pathway inhibitor: structure, biology and involvement in disease. The Journal of pathology. 2006; 208:327–339. [PubMed: 16261634]
14. White TA, Witt TA, Pan S, Mueske CS, Kleppe LS, Holroyd EW, Champion HC, et al. Tissue factor pathway inhibitor overexpression inhibits hypoxia-induced pulmonary hypertension. American journal of respiratory cell and molecular biology. 2010; 43:35–45. [PubMed: 19648471]
15. Wolberg AS. Thrombin generation and fibrin clot structure. Blood reviews. 2007; 21:131–142. [PubMed: 17208341]
16. Lenselink EA. Role of fibronectin in normal wound healing. International wound journal. 2013; 9999
17. Greiling D, Clark RA. Fibronectin provides a conduit for fibroblast transmigration from collagenous stroma into fibrin clot provisional matrix. Journal of cell science. 1997; 110(Pt 7): 861–870. [PubMed: 9133673]
18. Fiorucci S, Antonelli E, Distrutti E, Severino B, Fiorentina R, Baldoni M, Caliendo G, et al. PAR1 antagonism protects against experimental liver fibrosis. Role of proteinase receptors in stellate cell activation. Hepatology. 2004; 39:365–375. [PubMed: 14767989]
19. Wierzbicka-Patynowski I, Schwarzbauer JE. The ins and outs of fibronectin matrix assembly. Journal of cell science. 2003; 116:3269–3276. [PubMed: 12857786]
20. Lebray P, Varnous S, Charlotte F, Varaut A, Poynard T, Ratziu V. Liver stiffness is an unreliable marker of liver fibrosis in patients with cardiac insufficiency. Hepatology. 2008; 48:2089. [PubMed: 19003902]
21. Frulio N, Laumonier H, Balabaud C, Trillaud H, Bioulac-Sage P. Hepatic congestion plays a role in liver stiffness. Hepatology. 2009; 50:1674–1675. [PubMed: 19670411]
22. Wells RG, Discher DE. Matrix elasticity, cytoskeletal tension, and TGF-beta: the insoluble and soluble meet. Science signaling. 2008; 1:pe13. [PubMed: 18334714]
23. Olsen AL, Bloomer SA, Chan EP, Gaca MD, Georges PC, Sackey B, Uemura M, et al. Hepatic stellate cells require a stiff environment for myofibroblastic differentiation. American journal of physiology. Gastrointestinal and liver physiology. 2011; 301:G110–118. [PubMed: 21527725]
24. Cha SD, Desai RS, Gooch AS, Maranhao V, Goldberg H. Diagnosis of severe tricuspid regurgitation. Chest. 1982; 82:726–731. [PubMed: 7140400]
25. Sherlock S. The liver in heart failure; relation of anatomical, functional, and circulatory changes. British heart journal. 1951; 13:273–293. [PubMed: 14848381]
26. Neubauer K, Knittel T, Armbrust T, Ramadori G. Accumulation and cellular localization of fibrinogen/fibrin during short-term and long-term rat liver injury. Gastroenterology. 1995; 108:1124–1135. [PubMed: 7698580]
27. Beier JI, Luyendyk JP, Guo L, von Montfort C, Staunton DE, Arteel GE. Fibrin accumulation plays a critical role in the sensitization to lipopolysaccharide-induced liver injury caused by ethanol in mice. Hepatology. 2009; 49:1545–1553. [PubMed: 19291788]

28. Fraser R, Bowler LM, Day WA, Dobbs B, Johnson HD, Lee D. High perfusion pressure damages the sieving ability of sinusoidal endothelium in rat livers. British journal of experimental pathology. 1980; 61:222–228. [PubMed: 7426378]
29. Sechler JL, Corbett SA, Wenk MB, Schwarzbauer JE. Modulation of cellextracellular matrix interactions. Annals of the New York Academy of Sciences. 1998; 857:143–154. [PubMed: 9917839]
30. Wells RG. The role of matrix stiffness in regulating cell behavior. Hepatology. 2008; 47:1394–1400. [PubMed: 18307210]
31. Georges PC, Hui JJ, Gombos Z, McCormick ME, Wang AY, Uemura M, Mick R, et al. Increased stiffness of the rat liver precedes matrix deposition: implications for fibrosis. American journal of physiology. Gastrointestinal and liver physiology. 2007; 293:G1147–1154. [PubMed: 17932231]
32. Kolen AF, Miller NR, Ahmed EE, Bamber JC. Characterization of cardiovascular liver motion for the eventual application of elasticity imaging to the liver in vivo. Physics in medicine and biology. 2004; 49:4187–4206. [PubMed: 15509060]
33. Wright M, Goldin R, Hellier S, Knapp S, Frodsham A, Hennig B, Hill A, et al. Factor V Leiden polymorphism and the rate of fibrosis development in chronic hepatitis C virus infection. Gut. 2003; 52:1206–1210. [PubMed: 12865283]
34. Abe W, Ikejima K, Lang T, Okumura K, Enomoto N, Kitamura T, Takei Y, et al. Low molecular weight heparin prevents hepatic fibrogenesis caused by carbon tetrachloride in the rat. Journal of hepatology. 2007; 46:286–294. [PubMed: 17166617]
35. Yamanobe F, Mochida S, Ohno A, Ishikawa K, Fujiwara K. Recombinant human tissue factor pathway inhibitor as a possible anticoagulant targeting hepatic sinusoidal walls. Thrombosis research. 1997; 85:493–501. [PubMed: 9101641]
36. Akiyoshi H, Terada T. Centrilobular and perisinusoidal fibrosis in experimental congestive liver in the rat. Journal of hepatology. 1999; 30:433–439. [PubMed: 10190726]
37. Iwakiri Y. Endothelial dysfunction in the regulation of cirrhosis and portal hypertension. Liver international : official journal of the International Association for the Study of the Liver. 2012; 32:199–213. [PubMed: 21745318]

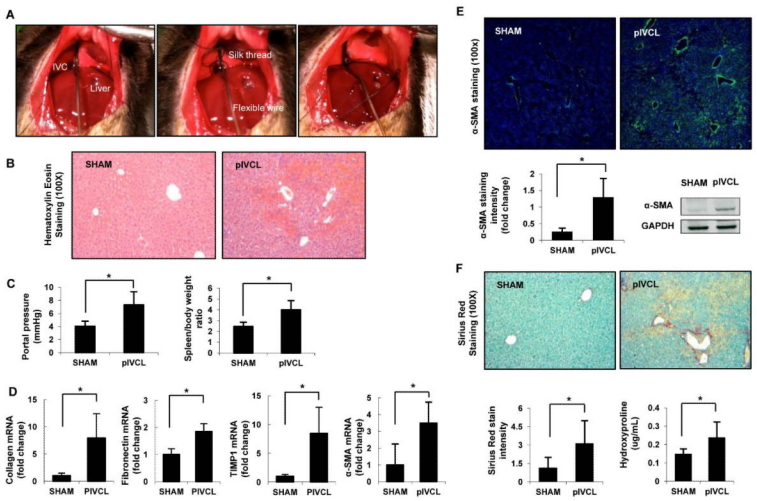

Figure 1. Characterization of a Murine Model of Congestive Fibrosis by Partial Ligation of the Inferior Vena Cava

Surgical model of congestive hepatopathy in C57BL/6 mice through partial ligation of the suprahepatic inferior vena cava (pIVCL) is shown (A). The IVC was circumferentially isolated and a sterile wire was placed on the anterior surface of the IVC (A, left). A 6.0 silk thread was then tightly tied around both the IVC and the wire (A, right), which was subsequently removed. Six weeks postoperatively livers were harvested and subjected to analysis. Hematoxylin-Eosin staining (100X) on paraffin sections demonstrate areas of centrilobular necrosis, vascular extravasation and sinusoidal dilatation (B). Portal pressure was directly measured via cannulation of portal vein and spleen/body ratio was calculated as a surrogate of portal hypertension (C). Hepatic expression of fibrogenic markers is increased after pIVCL compared to SHAM (D). Hepatic stellate cell activation after pIVCL is also demonstrated by increased α-SMA immunofluorescence (200X) and protein levels (E). Significant increase in hepatic fibrosis 6 weeks post-pIVCL is shown by Sirius red staining (100X) and hydroxyproline content (F). Data represent mean ± STDEV; n=8-9, *p<0.05.

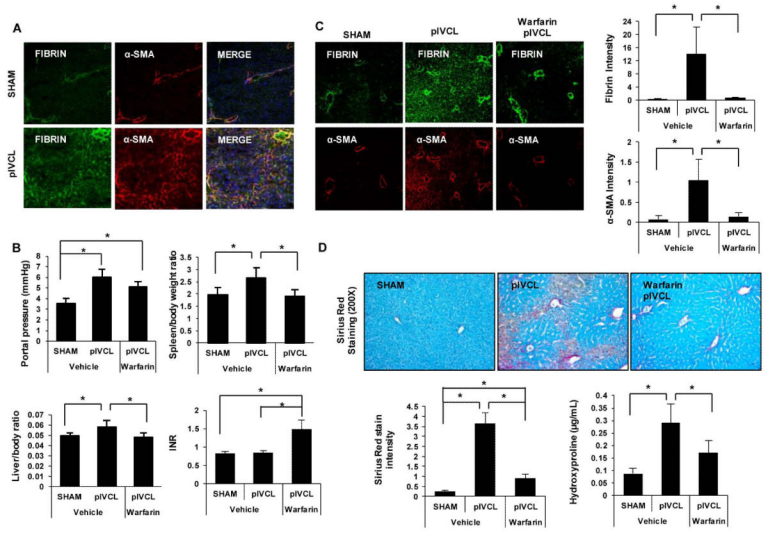

Figure 2. Anticoagulation Disrupts Congestive Fibrosis

Immunofluorescence for fibrin (green) was significantly increased in the liver after pIVCL compared to controls, and spatially associated with α-SMA expression (red) (200X) (A). Mice received warfarin (1 μg/mL) in drinking water post-pIVCL for 6 weeks until sacrifice. Control animals received plain water for 6 weeks. International normalized ratio (INR) of two times the controls was successfully achieved with this dosage (B, left upper panel). Portal pressure was measured and livers were perfused with 10 mL of 1X PBS through the portal vein to remove circulating fibrinogen. Spleen and liver were then harvested and body ratios calculated (B). Immunofluorescence for fibrin (green) and α-SMA (red) were significantly decreased with warfarin treatment (C). Warfarin-treated animals showed significant reduction in hepatic fibrosis compared to untreated pIVCL group (D). Data represent mean ± STDEV; n=10, *p<0.05.

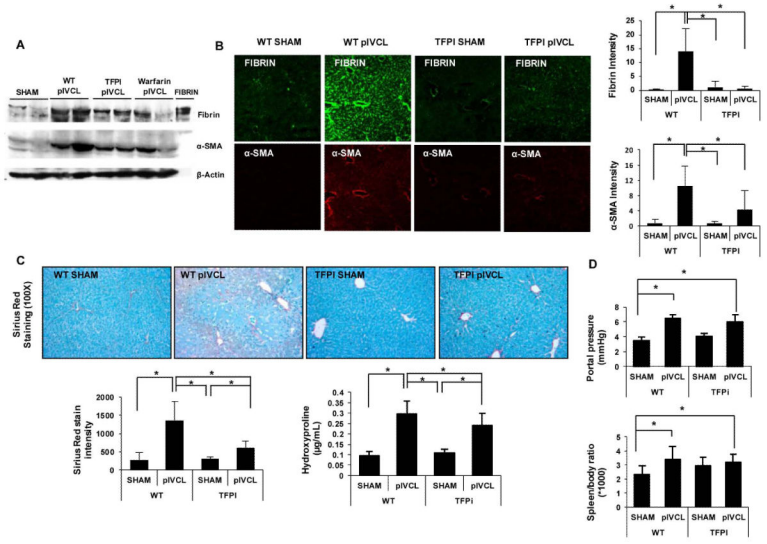

Figure 3. Tissue Factor Pathway Inhibitor Transgenic Mice Show Reduced Fibrosis after Partial IVC Ligation

Tissue factor pathway inhibitor (TFPI) overexpression was obtained via smooth muscle-specific promoter SM22α (SM22α-TFPI) in C57BL/6 mice, to achieve elevated systemic levels of TFPI. SM22α-TFPI mice were submitted to SHAM and pIVCL surgeries and wild type mice were used as controls. Western blot analysis is shown of fibrin, α-SMA and β-actin from liver lysates of SHAM and pIVCL in WT, SM22α-TFPI and warfarin-treated WT mice. Lysates are shown from two distinct mice from each group. Bovine fibrinogen (1 mg/ml) and thrombin (0.2 U/ml) were mixed to form fibrin *in vitro*, which was used as positive control (A). Fibrin (green) and α-SMA (red) immunofluorescence were reduced in SM22α-TFPI mice after pIVCL compared to wild type animals. Hepatic fibrosis was significantly reduced as demonstrated by sirius red staining and hydroxyproline assay (C). Portal pressure and spleen/body ratio were not affected by TFPI overexpression (D). Data represent mean ± STDEV; n=7-10, *$p<0.05$.

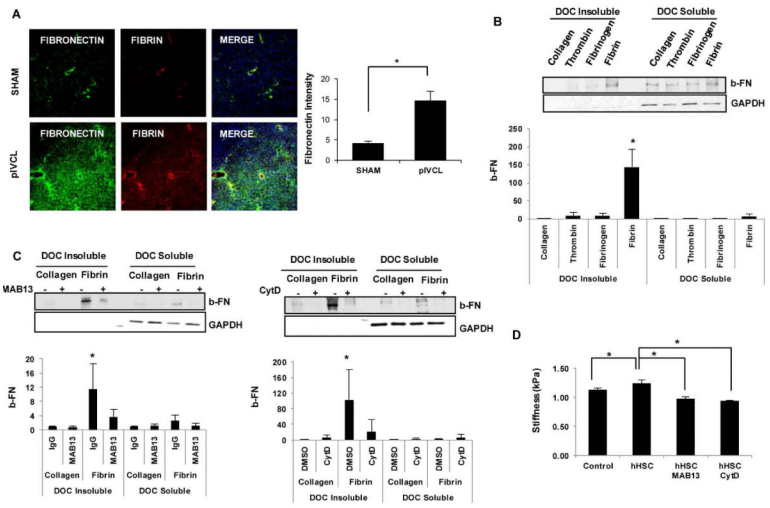

Figure 4. Fibrin Stimulates Fibronectin Fibril Assembly by HSC

Fibronectin (green) and fibrin (red) immunofluorescence were performed from frozen liver sections after 6 weeks of SHAM and pIVCL. Fibronectin significantly increased after pIVCL compared to SHAM and co-localized with fibrin at sites of congestion-related injury (A). Serum starved hHSC were plated on collagen-, fibrinogen- and fibrin-coated or uncoated dishes. Thrombin (0.2 U) was added to serum-free media of cells on uncoated dishes. Biotinylated fibronectin (10 μg) was added for 6 hours and cells were collected for deoxycholic acid (DOC) solubility assay as described on methods. Insoluble and soluble fractions were resolved on a 4–12% SDS-PAGE gel. GAPDH is shown as loading control. Fibrin significantly increased insoluble fraction of fibronectin compared to collagen, fibrinogen and thrombin (B). hHSC plated on fibrin- or collagen- coated dishes were pre-treated with rat anti-human CD29 (Mab13; 1:200) or cytochalasin D (1:1000) for 30 minutes prior to addition of b-FN. Mab13 and CytD significantly reduced assembly of exogenous fibronectin by hHSC in response to fibrin (C). Fibrin gels containing hHSC were constructed and Mab13 or CytD added to serum-free media. Fibrin gels with no cells were used as controls. MR elastography was obtained after 5 days for measurement of shear stiffness (kPa) (D). *In vitro* experiments were performed 3 times with similar results. Data represent mean ± STDEV; *$p<0.05$.

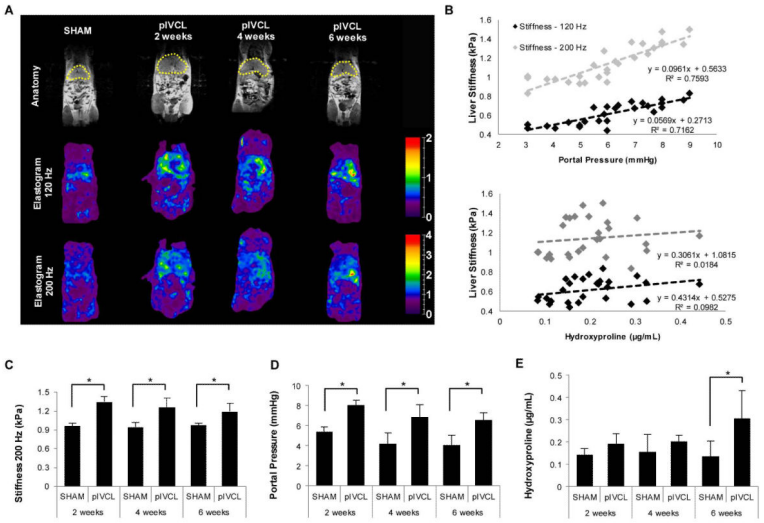

Figure 5. Liver Stiffness Correlates with Portal Hypertension in Congestive Hepatopathy

Mice underwent SHAM or pIVCL surgeries for 2, 4 or 6 weeks. On day of sacrifice, MR elastogram was performed using a custom birdcage coil. RE wave images were acquired with a multifrequency 3-D/3-axis EPI MRE sequence (120 and 200Hz) with a resolution of 0.3×0.3×2 mm3 (A). Yellow dashed line indicates total liver areas (upper panel). Portal pressure was directly measured, via cannulation of portal vein, and livers were harvested for hydroxyproline assay. Liver stiffness (kPa) correlated with portal pressure after pIVCL (R^2=0.7162 at 120Hz and R^2=0.7593 at 200Hz), to a much greater extent than with fibrosis as measured by hydroxyproline content (R^2=0.0982 at 120Hz and R^2=0.0184 at 200Hz) (B). Liver stiffness (C) and portal pressure (D) significantly increased after pIVCL at 2, 4 and 6 weeks compared to SHAM groups. Fibrosis was only significantly increased at 6 weeks after pIVCL compared to SHAM (E). Data represent mean ± STDEV; n=4-5, *p<0.05.

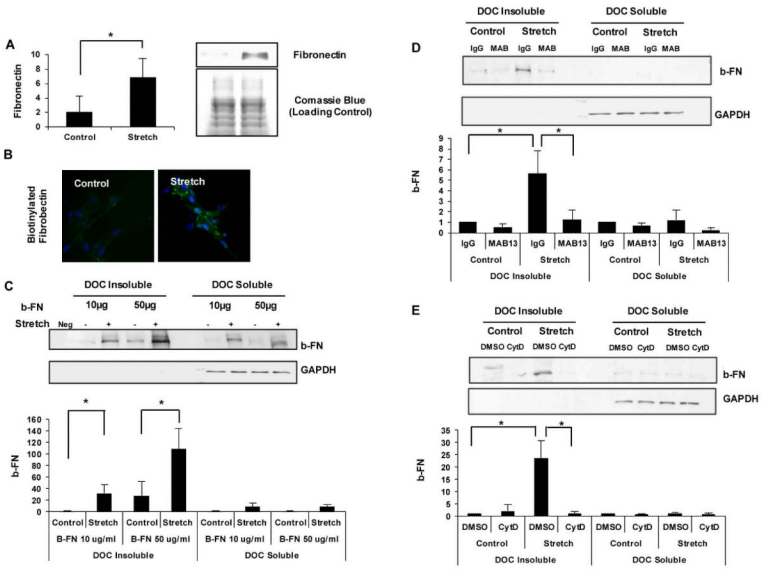

Figure 6. Mechanical Forces Stimulate Fibronectin Fibril Assembly by HSC

Primary human and murine HSC were seeded on 6-well plates of flexible silicone bottom coated with collagen type IV at 0.3 $\times 10^6$ cells/well. After incubation for 24 hours, cells were serum-starved overnight and then subjected to cyclic uniform stretch. Amplitudes of 10% strain were used at a rate of 30 cycles/min at 37 °C and 5% CO2 in a humidified incubator. Serum-starved HSCs were submitted to cyclic stretch for 24 hours. HSC supernatant were collected for western blot analysis of fibronectin. Comassie blue was used for loading control (A). Biotinylated fibronectin (10 µg) was added and cells were submitted to cyclic stretch for 6 hours. Streptavidin immunofluorescence (green) demonstrates deposition of b-FN fibrils on the surface of HSCs. Nucleus staining (DAPI) is in blue (B). b-FN at 10 and 50 µg/mL was added to serum-starved HSC. Cells were cyclic stretched for 6 hours and collected for DOC-solubility assay. Cyclic stretch significantly increased insoluble fibronectin compared to non-stretched cells (C). Pre-treatment with rat anti-human CD29 (Mab13; 1:200) or cytochalasin D (1:1000) for 30 minutes prior to cyclic stretch significantly reduced assembly of exogenous fibronectin by hHSC (D, E). Experiments were performed 3 times with similar results. Data represent mean ± STDEV; *$p<0.05$.

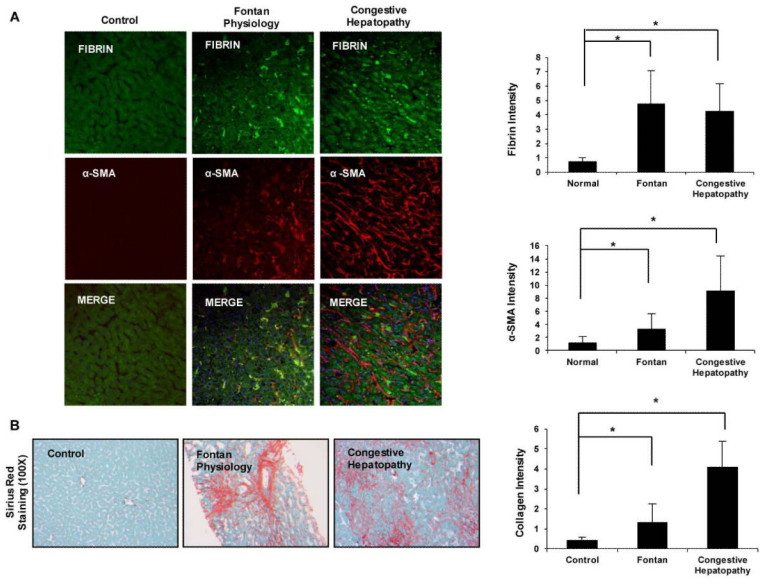

Figure 7. Intrahepatic Thrombosis is increased in Humans with Congestive Hepatopathy

Liver samples were obtained from healthy individuals (controls) and from patients with congestive hepatopathy secondary to congestive heart failure or corrective surgery (Fontan procedure) for complex congenital heart disease. Fibrin (green) and α-SMA (red) immunofluorescence are significantly increased in congestive hepatopathy compared to controls. Fibrosis is also significantly increased as demonstrated by Sirius red staining (n=20, controls; n=12, Fontan procedure; n=14, congestive heart failure). Patient demographics are shown in Supplementary Table 1 and 2. Data represent mean ± STDEV; *p<0.05.

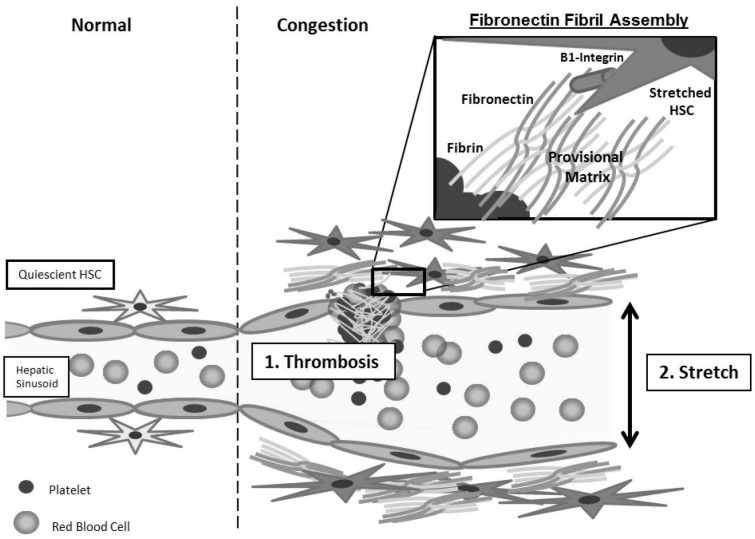

Figure 8. Proposed Model of Fibrosis Development in Congestive Hepatopathy

In chronic hepatic congestion, sinusoidal dilatation leads to stretch of adjacent hepatic stellate cells, and stasis promotes intravascular thrombosis with fibrin clot formation. Cyclic mechanical stretch induces release of fibronectin by HSC and both fibrin and stretch stimulate fibronectin fibril assembly via β1-integrin and actin-dependent mechanism.